Advanced Multi-Functional Model Predictive Control for Three-Phase AC/DC Converters

Xiaolong Shi[1], Jianguo Zhu[1], Dylan Dah-Chuan Lu[1], Li Li[1]
[1]School of Electrical, Mechanical and Mechatronic Systems, University of Technology, Sydney, Australia
Xiaolong.Shi@student.uts.edu.au

***Abstract*—With the conventional model predictive control (MPC) based direct power control of three-phase AC/DC converters, the active and reactive powers can be simultaneously controlled by a single cost function. A change in parameters of either the active or reactive power within the cost function will affect the other, leading to poor dynamic performance of transient response. Besides, the steady state performance of the conventional MPC is affected by one-step-delay of digital implementation. This paper proposes an advanced multi-functional MPC of three-phase full-bridge AC/DC converter for high power applications. It has multiple functions such as one-step-delay compensation, power ripple reduction, switching frequency reduction, and dynamic mutual influence elimination. Using the proposed modified cost function, both the steady state and dynamic performances of the converter can be improved. Finally, the simulation results are reported to validate the advancement of the proposed control strategy in comparison with other control methods.**

***Index Terms*—Direct power control, Cost function, AC/DC converter, Model predictive control**

I. Introduction

Nowadays, renewable energy sources are of vital importance to satisfy the energy consumption in the future. The three-phase full-bridge AC/DC converter is a popular option for integration of renewable energy sources and energy storage system (ESS) due to its advantages such as four quadrant power flow, input power factor correction, flexible DC-link voltage adjustment, and relatively low DC filter capacitance as compared with uncontrolled AC/DC converters. The fast development of renewable energy systems also leads to more stringent requirements of AC/DC converters, and more advanced control strategies that can deliver better system reliability and power quality.

The direct power control (DPC) and voltage-oriented control (VOC) are two typical advanced control methods [1], [2]. The VOC regulates the input active and reactive powers by controlling the input current. Although this method has good dynamics response and stability in the steady state, the inner current controller has large influence on system performance, whereas the DPC can control the active and reactive powers directly by selecting an appropriate space voltge vector from the preset switching table according to the instantaneous errors between the referenced and instantaneous values of active and reactive powers, and the voltage vector position.

Other control strategies, such as the space vector modulation control, model predictive control (MPC), and fuzzy logic based DPC, have also attracted much attention in recent years. Among them, MPC is a flexible control method that allows easy inclusion of system nonlinearities and constraints [3]-[5]. In the MPC based DPC control scheme, the system model and cost function of errors between the reference and current active and reactive powers are evaluated for a finite set of voltage space vectors, and the voltage space vector that can minimize the cost function is selected for actuation.

The control objectives of cost function can vary relatively according to different applications. For example, the conventional MPC method has one-step delay influence due to digital implementation. The concept of multi-objective control was proposed to compensate the one-step-delay while keeping the system stability and achieving switching frequency reduction [6]. This approach however only contributes to improving the system steady state performance. During the transient state, if one control objective experiences a large change in the power reference (either active or reactive power), the control weight is focused on the changed objective, and then the voltage vector that is more likely to adjust the objective to reference value would be selected according to the cost function. This influences the control of the other control target since these two control objectives could not be totally decoupled according to the converter model, and thus deteriorates the dynamic performance. This problem is more likely to occur particularly in higher power system. An improved MPC cost function was proposed in [7] to eliminate this mutual influence. However, the steady state performance was compromised.

In order to solve this issue, this paper proposes an advanced MPC to improve both the dynamic and steady state performances simultaneously by adding multiple control objectives in the cost function to consider the dynamic and steady state performance simultaneously. The new method can improve not only the steady state performance by one step delay compensation while solving the corresponding system deterioration issue such as

switching frequency increment, but also the dynamic performance by adding more system constraints to compensate the mutual influence between the active and reactive power references in the cost function.

II. Modeling of Three Phase Converter

Fig.1 illustrates the topology of a three phase AC/DC converter that can be operated for bi-directional power conversion. Fig.2 shows a diagram showing the voltage space vectors.

The three phase IGBT bridge unit is connected to either the main grid or an AC load via a choke consisting of three series-connected inductors L and resistors R. At the DC side, a DC load or DC bus is connected to the IGBT bridge in parallel to a capacitor C, where e_a, e_b, and e_c are the three-phase AC source voltages; v_a, v_b, and v_c the AC terminal voltages of the three phase bridge; and i_a, i_b, and i_c the three-phase currents.

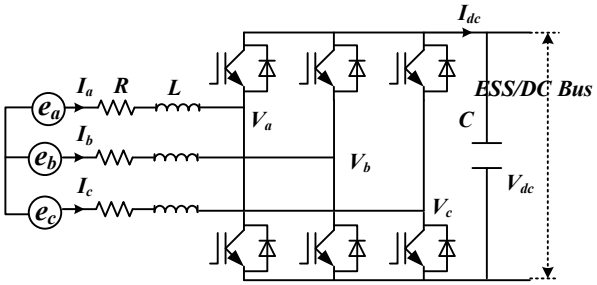

Fig.1 AC/DC three-phase converter structure

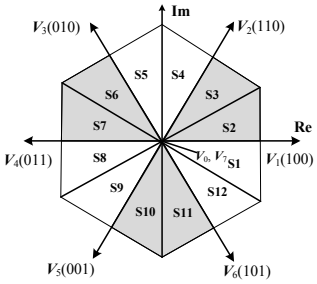

Fig.2 Voltage space vectors

In the stationary reference frame, the AC source voltage vector and current vector in the αβ-coordinate system can be calculated by following transformation:

$$e_{\alpha\beta} = \begin{bmatrix} e_\alpha \\ e_\beta \end{bmatrix} = \frac{2}{3}\begin{bmatrix} 1 & -1/2 & -1/2 \\ 0 & \sqrt{3}/2 & -\sqrt{3}/2 \end{bmatrix}\begin{bmatrix} e_a \\ e_b \\ e_c \end{bmatrix} \tag{1}$$

$$I_{\alpha\beta} = \begin{bmatrix} I_\alpha \\ I_\beta \end{bmatrix} = \frac{2}{3}\begin{bmatrix} 1 & -1/2 & -1/2 \\ 0 & \sqrt{3}/2 & -\sqrt{3}/2 \end{bmatrix}\begin{bmatrix} I_a \\ I_b \\ I_c \end{bmatrix} \tag{2}$$

In a balanced three-phase system, the line currents can be calculated in the stationary reference frame as follows:

$$e_{\alpha\beta} = L\frac{dI_{a\beta}}{dt} + RI_{a\beta} + V_{\alpha\beta} \tag{3}$$

$$C\frac{dV_{dc}}{dt} = \frac{3}{2}\left(I_\alpha S_\alpha + I_\beta S_\beta\right) - I_L \tag{4}$$

where $\boldsymbol{e}_{\alpha\beta}$, $\boldsymbol{V}_{\alpha\beta}$, $\boldsymbol{I}_{\alpha\beta}$, and I_L are the input source voltage vector, the three-phase converter input voltage vector, the line current vector, and load current, respectively. The active and reactive power exchange with the grid can be calculated as

$$\begin{bmatrix} P \\ Q \end{bmatrix} = \frac{3}{2}\begin{bmatrix} e_\alpha & e_\beta \\ e_\beta & -e_\alpha \end{bmatrix}\begin{bmatrix} I_\alpha \\ I_\beta \end{bmatrix} \tag{5}$$

III. Predictive Model of AC/DC Converter

The conventional DPC (CDPC) scheme is based on the instantaneous active and reactive powers to form the control loops, as described in [1]. The voltage vector of the PWM rectifier is chosen from a preset switching table. It is formulated according to the digitized signals S_p and S_q from the tracking errors of active and reactive powers, respectively, which are provided according to a fixed band hysteresis comparators and the power source voltage vector position, θ_n, in the α–β plane. Since CDPC is a very popular control strategy, it will be compared with the proposed control scheme in this paper.

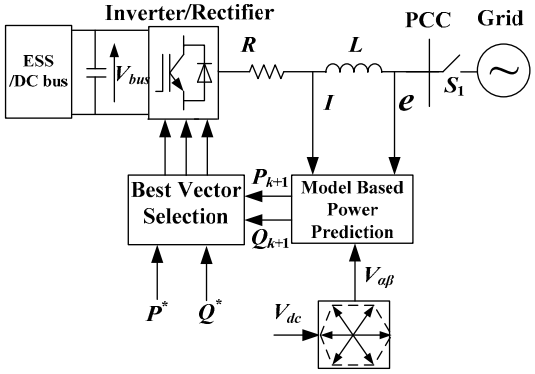

Fig.3 Block diagram of MPC-based power regulation

The MPC based DPC predicts the change of power behavior at the time instant (k+1) for different voltage vectors and apply the voltage vector that has the minimum power ripple. Fig.3 illustrates the block diagram of MPC. The differential equation matrix of active and reactive powers can be derived from (3) and (4) as

$$\frac{d}{dt}\begin{bmatrix} P \\ Q \end{bmatrix} = \frac{3}{2}\left(I_\alpha \frac{d}{dt}\begin{bmatrix} e_\alpha \\ e_\beta \end{bmatrix} + \frac{dI_\alpha}{dt}\begin{bmatrix} e_\alpha \\ e_\beta \end{bmatrix} + I_\beta \frac{d}{dt}\begin{bmatrix} e_\beta \\ -e_\alpha \end{bmatrix} + \frac{dI_\beta}{dt}\begin{bmatrix} e_\beta \\ -e_\alpha \end{bmatrix}\right) \tag{6}$$

For the sinusoidal and balanced three phase line voltage,

$$\vec{e} = e_\alpha + je_\beta = |\vec{e}\,|\,e^{j\omega t} \tag{7}$$

From (7), the following expression can be deduced as

$$\frac{d}{dt}\begin{bmatrix} e_\alpha \\ e_\beta \end{bmatrix} = \omega \cdot \begin{bmatrix} -e_\beta \\ e_\alpha \end{bmatrix} \tag{8}$$

The instantaneous active and reactive powers can be derived by substituting (1) and (8) into (6) as

$$\frac{d}{dt}\begin{bmatrix} P_i \\ Q_i \end{bmatrix} = -\frac{R}{L}\begin{bmatrix} P_i \\ Q_i \end{bmatrix} + \omega\begin{bmatrix} -Q_i \\ P_i \end{bmatrix} + \frac{3}{2L}\begin{bmatrix} \left(|\vec{e}|^2 - \mathrm{Re}\left(\vec{e}\vec{V}_i^*\right)\right) \\ -\mathrm{Im}\left(\vec{e}\vec{V}_i^*\right) \end{bmatrix} \quad (9)$$

where $\vec{V}_i$ represents the voltage space vector. For every switching state and the corresponding voltage space vector, $V_{i\alpha}$ and $V_{i\beta}$ are calculated as follows,

$$\begin{bmatrix} V_{i\alpha} \\ V_{i\beta} \end{bmatrix} = \frac{2}{3}V_{dc}\begin{bmatrix} S_{ia} - \frac{1}{2}(S_{ib} + S_{ic}) \\ \frac{\sqrt{3}}{2}(S_{ib} - S_{ic}) \end{bmatrix} \quad (10)$$

where S_{ia} , S_{ib} and S_{ic} are the switching states of the converter.

If the tracking error of the DC-bus voltage is assumed constant over two successive sampling periods, the instantaneous active power at the next sampling instant (k+1) can be estimated using a linear extrapolation [8]. Thus, at the end of sampling period T_s, the predictive active and reactive powers for each converter switching state can be expressed as:

$$\begin{bmatrix} P_i^{k+1} \\ Q_i^{k+1} \end{bmatrix} = T_s\left(-\frac{R}{L}\begin{bmatrix} P_i^k \\ Q_i^k \end{bmatrix} + \omega\begin{bmatrix} -Q_i^k \\ P_i^k \end{bmatrix} + \frac{3}{2L}\begin{bmatrix} \left(|\vec{e}|^2 - \mathrm{Re}\left(\vec{e}\vec{V}_i^*\right)\right) \\ -\mathrm{Im}\left(\vec{e}\vec{V}_i^*\right) \end{bmatrix}\right) + \begin{bmatrix} P_i^k \\ Q_i^k \end{bmatrix} \quad (11)$$

The system can compare the active and reactive powers of each converter switching state, and chose the one leading to the least power ripple according to the specific cost function defined as

$$J_i = \sqrt{(P^* - P_i^{k+1})^2 + (Q^* - Q_i^{k+1})^2} \quad (12)$$

IV. Advanced MPC Control for Steady and Dynamic Performance Optimization

One of the main advantages of MPC is that any variable and constraint term or requirement of the system for a prediction could be added in the cost function to combine multiple constraints and nonlinearities to improve the system performance. The conventional MPC has two main issues which may influence the system performances. The first one is the influence of one-step delay, which could cause large power ripples deteriorating the system steady state performance. The second one is the dynamic mutual influence of active power and reactive powers, deteriorating the system dynamic performance. The control design of the proposed advanced MPC method is illustrated schematically in Fig.4. With the redesigned cost function and additional constraints, the proposed advanced MPC control could improve both the steady state and dynamic performance of the three-phase converter, simultaneously, in comparison with the conventional MPC control. For different control aspects, the key is to choose the correct weighting factors to get a reasonable tradeoff between the various control objectives.

A. Steady state performance comparisons

- One-step-delay compensation

In the steady state operation, the most significant influence is caused by the one-step-delay in discrete-time digital implementation [9], as shown in Fig. 4. The one-step-delay issue exists when using (11) and (12) for real system control, which increases system power ripples in the steady state, and causes errors in power prediction. Take the active power as an example. As illustrated in Fig. 5, P^k is sampled at *kth* instant, and T_c the computing time of control strategy. After the best voltage vector V_i^{k+1} is determined using P^k and P^*, it will be applied at the (k+1)th instant while the active power variables at the (k+1)th instant is changed to P^{k+1}, which would be usually different from P^k because of the application of V_i^k. Therefore, the vector chosen at the (k+1)th instant may no longer be the best one, the one step ahead prediction value P^{k+2} that acquired through the converter model should be used in the cost function instead of P^{k+1} to calculate the best vector for (k+1)th instant. Likewise, the Q^{k+2} acquired through the prediction model should be used in cost function instead of Q^{k+1} for best vector selection.

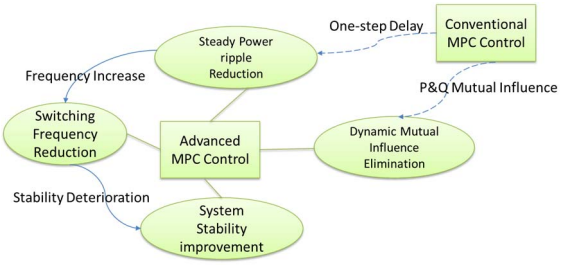

Fig.4 Advanced control design in comparison with CMPC

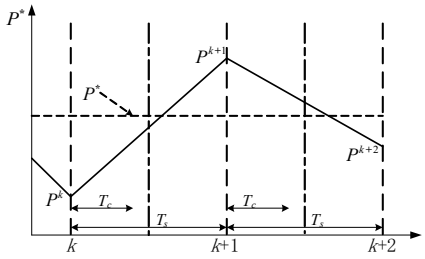

Fig.5 Data processing in digital implementation.

With the one-step-delay compensation, the cost function should be redefined as

$$J_i = (P^* - P_i^{k+2})^2 + (Q^* - Q_i^{k+2})^2 \quad (13)$$

- Switching frequency reduction

While applying the one-step-delay compensation, the switching frequency increases significantly. The power losses of the converter increase with the increase of switching frequency, especially in high power applications. The switching frequency can be reduced by obtaining the minimum possible state changes of each switch [6]. Take the switching state “000” as an example. Fig. 6 shows the

possible vector switching patterns. It can be seen that there are four patterns according to the number of switches; i.e. the zero, one-state, two-state, and three-state changes. To reduce the switch state change, the switching path which has least leg switch changes is preferred.

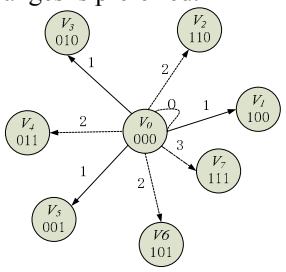

Fig.6 Switching paths of vectors.

According to the analyses above, the cost function (13) can be further revised to

$$J = (P^* - P_i^{k+2})^2 + (Q^* - Q_i^{k+2})^2 + \lambda_1 \left(\sum_{i=a,b,c} \left| D_i^{k+1} - D_i^k \right| \right) \quad (14)$$

where D_i^k and D_i^{k+1} represent the switching state of phase i (i=a, b, c) bridge leg in the current and the following control periods, respectively. D_i^k = 0 or 1, where 1 means that the upper switch is on and the lower one is off, and 0 the reverses switching state. λ_1 is the weighting factor. Therefore, by redesigning the cost function as (14), the switching frequency reduction can be realized.

- System stability improvement

The system control stability will deteriorate with the application of switching frequency reduction method, resulting in quite large power and current ripples. A solution is introduced in [6] to predict the behavior of the variables with N steps ahead, by controlling the tracking error at the N (N >1) instants. This could help to reduce the system power ripples, especially when λ_1 is too large. The active and reactive powers at the (k+N)th instant is predicted linearly from the value at the (k+1)th and (k+2)th instants.

Finally, for the steady state performance improvement, the cost function (14) can be further revised to

$$J = (P^* - P_i^{k+2})^2 + (Q^* - Q_i^{k+2})^2 + \lambda_1 \left(\sum_{i=a,b,c} \left| D_i^{k+1} - D_i^k \right| \right) + \lambda_2 \left(\left| P^* - P_i^{k+N} \right| + \left| Q^* - Q_i^{k+N} \right| \right) \quad (15)$$

which is same as that in [6], where λ_2 is the weighting factor of system stability, P_i^{k+N} and Q_i^{k+N} are the active and reactive powers at the (k+N)th instant using the linear extrapolation for the prediction horizon. However, till this stage with the revised cost function (15), only the steady state performance is improved while the dynamic performance has not been considered.

B. Dynamic state performance comparisons

In the aforementioned MPC control cost functions, the control objectives, namely the active and reactive power, are combined into one cost function and are controlled at the same time by achieving the minimum cost function value. If one objective significantly changes in a large-scale system using MPC control with the aforementioned cost function, the control target is focused on the changed objective, while the other objective is less controlled and the dynamic performance would deteriorate. The interaction becomes larger while the variation amount of the two control factors becomes larger. Due to such influence, the issue of dynamic performance deterioration should be taken into account.

To eliminate the mutual interference issue and enhance the dynamic state performance of the conventional MPC, the cost function (15) for improving steady performance is further reorganized. Adding the weighting factor in the cost function to minimize the mutual interference results in the revised final cost function as

$$J = \lambda_P (P^* - P_i^{k+2})^2 + \lambda_Q (Q^* - Q_i^{k+2})^2 + \lambda_1 \left(\sum_{i=a,b,c} \left| D_i^{k+1} - D_i^k \right| \right) + \lambda_2 \left(\left| P^* - P_i^{k+N} \right| + \left| Q^* - Q_i^{k+N} \right| \right) \quad (16)$$

$$\lambda_p = \lambda \left| Q^* - Q^{k+2} \right| / Q_{rated} + 1$$

$$\lambda_Q = \lambda \left| P^* - P^{k+2} \right| / P_{rated} + 1$$

where λ_p and λ_Q are the parameters for eliminating the mutual influence, P^* is the active power reference value, Q^* the reactive power reference value, P_{rated} the rated active power, Q_{rated} the rated reactive power, λ the weighting factor for adjusting the amount of the parameters, and the optimal value of λ can be adjusted according to the system power level and parameters. For instance, when the active power changes significantly, the weighting factor λ_Q increases dramatically in comparison with λ_p for compensating the control weight of the reactive power. The same happens for the reactive power change.

In (16), each term has a corresponding weighting factor. By selecting proper weighting factors, the dynamic and steady state performance can be enhanced.

This is the first time for implementation of steady state and dynamic performance improvement at the same time. The proposed advanced MPC method chooses the voltage vector according to error amount of cost function taking the dynamic performance and steady performance into account simultaneously, the effects of each voltage vector on active and reactive power regulation will then be evaluated and applies the selected voltage vector that has minimum cost function result to the system.

V. SIMULATION RESULTS

The conventional DPC and MPC, as well as the proposed advanced MPC-DPC with multi-functions for bi-directional power flow have been numerically simulated using MATLAB/Simulink for the converter as shown in Fig.1. The main electrical parameters used in the simulation are

listed in Table I. The reference DC voltage V_{dc}^* is set to be 300 V.

TABLE I ELECTRICAL PARAMETER OF POWER CIRCUIT

Resistance of reactor	R	500 mΩ
Inductance of reactor	L	4.2 mH
DC-bus capacitor	C	1000 uF
Load resistance	R_L	50 Ω
Source voltage	e	110 V(peak)
Source voltage frequency	f	50 Hz
DC-bus voltage	V_{dc}	300 V

For simplicity, the conventional DPC method is denoted as "CDPC" and the conventional MPC based DPC methods without using one-step-delay compensation as "CMPC", the improved MPC with one-step-delay compensation as "IMPC", and the proposed advanced MPC as "AMPC".

For convenience, the power flow from the AC power supply to the DC load is defined as positive. To analyze both the steady state and dynamic performances for each of the control strategies, the active power reference value steps down from 0 W to -5000 W at 0.02 s while the reactive power reference remains 0 Var. After that, while the active power remains -5000 W, the reactive power decreases to -4000 Var at 0.04 s. At 0.06 s, the active power changes from -5000 W to 8000 W, while the reactive power returns to 0 Var at 0.08 s. At 0.1 s, the active power decreases from 8000 W to 2000 W.

A. Steady state performance comparisons

To compare the steady state performance, the AC three-phase input current and reactive power of the system are depicted from 0.03 s to 0.07 s to show the detailed power ripples. As we can see from Figs.7 and 8, both the active and reactive powers track their reference values with good accuracy and stability with four control methods.

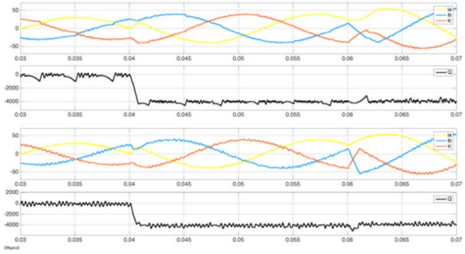

Fig. 7. From top to bottom, CDPC three-phase currents, CDPC reactive powers, CMPC three-phase currents, CMPC reactive powers;

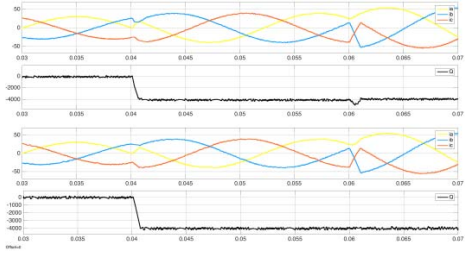

Fig.8. From top to bottom, IMPC three-phase currents, IMPC reactive powers, AMPC three-phase currents, AMPC reactive powers;

Take the 0.045 s to 0.005 s as an example. The reactive power ripple of CDPC is as high as 280.38Var and active power ripple is 209.52 W. In comparison, the reactive power ripple of CMPC is significantly reduced to be around 200.43 Var. The active power ripple decreases to 162.96 W, and the current waveform is more sinusoidal compared with the CDPC control. With the IMPC control, the power ripple of reactive power is less than 83.55 Var, and the active power ripple is around 91.14 W, which is the best performance in the steady state. With the AMPC control, the ripples of active and reactive powers in the steady state are almost the same as IMPC control, which is as expected.

In conclusion, in the steady state, both the IMPC and AMPC control methods have the best performance with lower active power and reactive power ripple.

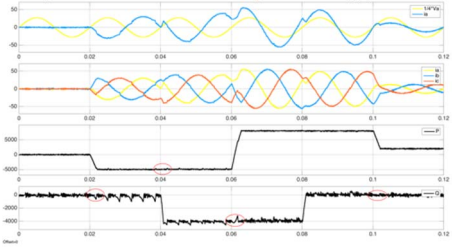

Fig.9. Simulated performance of CDPC. From top to bottom, AC voltage, three-phase currents, Active and reactive powers;

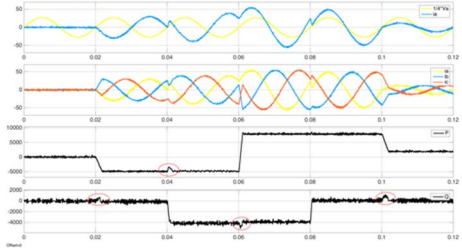

Fig.10. Simulated performance of CMPC. From top to bottom, AC voltage, three-phase currents, Active and reactive powers;

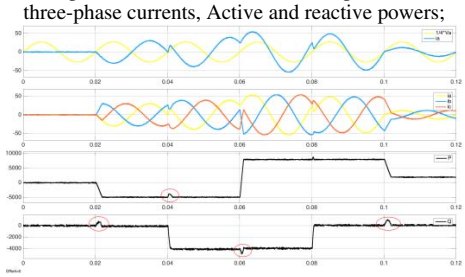

Fig.11 Simulated performance of IMPC. From top to bottom, AC voltage, three-phase currents, Active and reactive powers;

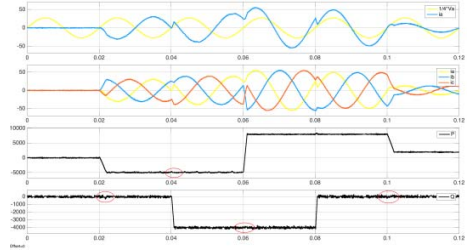

Fig.12. Simulated performance of AMPC. From top to bottom, AC voltage, three-phase currents, Active and reactive powers;

B. Dynamic state performance comparisons

To compare the dynamic state performance, the comparison of step change of active power and reactive power with four methods are conducted. With step-change

conditions, the sector where the mutual interference occurs is marked in dashed circles. In the transient state, there is no mutual influence between the active and reactive powers with the CDPC control. As shown in Fig.9, the active power tracks its reference with good approximation and stability. It takes 0.028 s when the active power steps up from -5000 W to 8000 W. In comparison, the mutual influence of active and reactive powers with the CMPC and IMPC are apparent when there are step changes of active and reactive powers during dynamic instants, as shown in dashed circles in Figs.10 and 11. For instance, the active power change can be as high as 1800 W at the instance when reactive power decreases from 0 W to -4000 W. The reactive power change can be 1200 Var when active power steps down from 8000 W to 2000 W at 0.1 s. However, compared with CDPC, it shows much better reference tracking ability and takes 0.001 s to track the active power reference when the active power steps up from -5000 W to 8000 W.

With AMPC method, the mutual influence between active and reactive powers is eliminated, as shown in Fig. 12. There is almost no overshoot of both reactive and active powers at step-change conditions in comparison with CMPC and IMPC methods, while retaining the same tracking ability as the CMPC and IMPC methods.

It can be concluded from these results that the proposed AMPC is the best one among these control methods in regard to the steady state and dynamic state performance.

C. *Switching frequency comparisons*

With the MPC control, the switching frequency increases apparently, which correspondingly increases the system costs. To compare the switching frequency reduction performance of different kinds of MPC methods, the switching frequency of each MPC control can be evaluated by counting the total state changes of one phase leg in a fixed period and divided by 2, which is shown in Fig. 13. The sample period of frequency calculation is every 0.01 s.

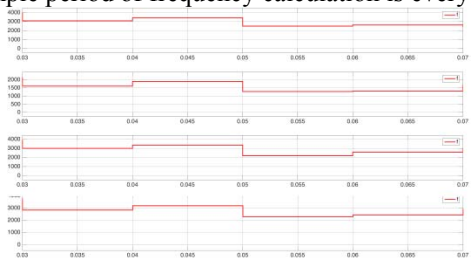

Fig.13. Switching frequency of system. From top to bottom, CMPC, CMPC with one-step-delay compensation, IMPC, AMPC

As shown in Fig. 13, all these control methods have variable frequency. From top to bottom are the switching frequency of CMPC control, CMPC control with additional one-step-delay compensation, IMPC control, and AMPC control. It can be seen that the CMPC control has the minimum frequency during whole simulation period in comparison with other methods. With only additional one-step-delay compensation of CMPC, the switching frequency increases significantly. With AMPC control, the switching frequency is further slightly decreased compared with IMPC, which verify that AMPC has switching frequency reduction ability compared with CMPC. The quantitative comparison is given in Table II. It should be noted that the response and overshoot of Q at 0.06 s instant as example while P has a step change. The switching frequency comparison was conducted at 0.045 s as example.

TABLE II Quantitative Comparison of System Performance

Control	*THD (%)*	*Prip* (W)	*Qrip* (Var)	*fsw* (Hz)	*Overshoot* (Var)	*Response (S)*
CDPC	7.2	209.5	280.4	3419	860	0.0029
CMPC	5.8	163.0	200.5	1902	1090	0.0012
IMPC	2.88	91.14	83.55	3350	990	0.0012
AMPC	2.83	92.6	83.3	3183	95	0.0012

VI. CONCLUSION

This paper proposes an advanced MPC strategy of three-phase AC/DC converters for improving the st and dynamic performances. Using MATLAB/Simulink, the steady state and dynamic performances of CDPC, CMPC, IMPC and AMPC for bi-directional power flow control of an AC/DC converter are simulated and compared. The simulation results verify the superior dynamic and steady state performance of the proposed AMPC method in comparison to other methods by reducing power ripples and eliminating the mutual influence between the active and reactive powers during the step-change instant, while retaining the switching frequency reduction ability.

REFERENCES

[1]. J. Hu, J. Zhu, and D. G. Dorrell, "A Comparative Study of Direct Power Control of AC/DC Converters for Renewable Energy Generation," in *Proc. IEEE IECON Conf.,* pp. 3453–3458, 2011.

[2]. J. Alonso-Martinez, J. Eloy-Garcia, and S. Arnaltes, "Table-based direct power control: A critical review for microgrid applications," *IEEE Trans. Power Electron.,* vol. 25, no. 12, pp. 2949-2916, December 2010.

[3]. M. Preindl, E. Schaltz, and P. Thogersen, "Switching frequency reduction using model predictive direct current control for high-power voltage sources inverters," *IEEE Trans. Ind. Electron.,* vol. 58, no. 7, pp. 2826-2835, July 2011.

[4]. S. A. Larrinaga, M. A. Rodriguez, E. Oyarbide and J. R. T. Apraiz, "Predictive control strategy for DC/AC converters based on direct power control," *IEEE Trans. Ind. Electron.,* vol. 54, pp. 1261-1271, June 2007.

[5]. S. Kouro, P. Cortes, R. Vargas, U. Ammann and J. Rodriguez, "Model predictive control─A simple and powerful method to control power converters," *IEEE Trans. Ind. Electron.,* vol. 56, no. 6, pp. 1826-1838, June 2009.

[6]. J. Hu, J. Zhu, G. Platt, and D. G. Dorrell, "Multi-objective model-predictive control for high power converters," *IEEE Trans. Energy Convers.,* vol. 28, no. 3, pp. 652-663, Sep. 2013.

[7]. D. Choi, K. Lee, "Dynamic performance improvement of AC/DC converter using model predictive direct power control with finite control set." *IEEE Trans. Ind. Electron.,* vol. 62, pp. 757-767, 2015.

[8]. H. Zhang and R. P. Paul, "A parallel inverse kinematics solution for robot manipulators based on multiprocessing and linear extrapolation," *IEEE Trans. Robotics Automat.,* vol. 7, no. 5, pp. 660-669, October 1991.

[9]. P. C. Loh, M. J. Newman, D. N. Zmood, and D. G. Holmes, "A comparative analysis of multiloop voltage regulation strategies for single and three-phase UPS systems," *IEEE Trans. Ind. Electron.,* vol. 18, no. 5, pp. 1176-1185, Sep. 2003.